

Title	Solution-processed silicon films and transistors
Author(s)	Shimoda, Tatsuya; Matsuki, Yasuo; Furusawa, Masahiro; Aoki, Takashi; Yudasaka, Ichio; Tanaka, Hideki; Iwasawa, Haruo; Wang, Daohai; Miyasaka, Masami; Takeuchi, Yasumasa
Citation	Nature, 440(7085): 783-786
Issue Date	2006-04-06
Type	Journal Article
Text version	author
URL	http://hdl.handle.net/10119/4880
Rights	This is the author's version of the work. Copyright (C) 2006 Nature Publishing Group. Tatsuya Shimoda, Yasuo Matsuki, Masahiro Furusawa, Takashi Aoki, Ichio Yudasaka, Hideki Tanaka, Haruo Iwasawa, Daohai Wang, Masami Miyasaka and Yasumasa Takeuchi, Nature, 440(7085), 2006, 783-786. http://dx.doi.org/10.1038/nature04613
Description	

Solution-Processed Silicon Films and Transistors

Tatsuya Shimoda,^{1*} Yasuo Matsuki,^{2*} Masahiro Furusawa,^{1*} Takashi Aoki,¹ Ichio Yudasaka,¹ Hideki Tanaka,¹ Haruo Iwasawa,² Daohai Wang,² Masami Miyasaka,¹ Yasumasa Takeuchi^{2†}

¹*Technology Platform Research Centre, Seiko Epson Corporation, 281 Fujimi, Fujimimachi, Nagano-ken, 399-0293 Japan.*

²*Fine Electronic Research Laboratories, JSR Corporation, 100 Kawajiri-cho, Yokkaichi, Mie, 510-8552 Japan.*

**These authors contributed equally to this work.*

† Present address: International Centre for Material Research, 1-1 Minamiwataridacho, Kawasaki-ku, Kawasaki-city, Kanagawa 210-0855 Japan.

Solution processes for electronic devices, instead of conventional vacuum process and vapour deposition, have been receiving considerable attention for a wide range of applications such as electroluminescent displays^{1,2}, solar cells³, ferroelectric films⁴, transparent conductive films⁵, SiO₂ films⁶ and metal films⁷, to reduce the processing cost. In particular, printing semiconductor devices using liquid materials is considered to be important for new applications, such as large-area flexible displays. Recent research has been focused on organic semiconductors⁸⁻¹¹, which have mobilities comparable to that of amorphous silicon (α -Si)¹¹, but are insufficiently reliable. Solution processing of metal chalcogenide semiconductors to fabricate stable and high-performance transistors has also been reported^{12,13}. This class of materials is targeted as substitutions for the silicon devices that require complex and expensive manufacturing processes. However, if high-quality silicon film could be prepared by solution process, this situation would change drastically. Here we demonstrate the solution process of silicon thin film transistors (TFTs) using a novel liquid precursor. We have formed poly-crystalline silicon (poly-Si) films by spin-coating or by ink-jetting the precursor to fabricate TFTs that operated with a mobilities of $108 \text{ cm}^2\text{V}^{-1}\text{s}^{-1}$ and $6.5 \text{ cm}^2\text{V}^{-1}\text{s}^{-1}$, respectively. These values cannot be achieved by solution-processed organic TFTs or α -Si TFTs, whose mobility is $1 \text{ cm}^2\text{V}^{-1}\text{s}^{-1}$ at most.

We have pursued the development of a novel liquid precursor (referred herein as "liquid silicon material") that can be used in a liquid process to form a silicon film^{14,15}. Since the films produced from this precursor must be convertible to high purity silicon, potential candidates are limited to carbon- and oxygen-free hydrogenated silicon compounds. Typical hydrogenated silicon compounds are either the straight-chain ($\text{Si}_n\text{H}_{2n+2}$) or cyclic (Si_nH_{2n}) compounds. For $n \geq 3$, these compounds are liquid at room temperature and decompose to form α -Si when heated to 300°C or higher. However, for $n < 10$, boiling points are less than 300°C and such compounds evaporate prior to thermal

decomposition making solution processing difficult. Oligomeric and polymeric hydrogenated polysilanes, $-(\text{SiH}_2)_n-$, because of limited solubility in organic solvents, have received little attentions since first being synthesized by Kipping method^{16, 17}. Nevertheless, hydrogenated polysilanes are potentially ideal liquid silicon materials provided a suitable solvent could be found. Because cyclic silanes are known to undergo ring-opening polymerisation^{18, 19}, this reaction can be utilized for the development of liquid silicon materials. We have applied photo-induced ring-opening polymerisation to obtain pure hydrogenated polysilanes from purified hydrogenated cyclic silanes. Among hydrogenated cyclic silanes, we chose cyclopentasilane (CPS), Si_5H_{10} , since it is relatively stable and exhibits a high photoreactivity when irradiated with ultraviolet (UV) light.

Using the method developed by Hengge *et al*^{20, 21}, CPS monomer, a clear and colourless liquid under ambient conditions, was synthesized. It has a boiling point of 194°C and is soluble in most organic solvents. After purification, the CPS was exposed to 405-nm UV light to induce photo-polymerisation. During exposure, the CPS gradually became cloudy and viscous. After sufficient exposure to the UV source, the liquid was transformed into a white solid, presumably a mixture of hydrogenated polysilanes. Although this solid is insoluble in all common organic solvent, it proved to be soluble in the CPS monomer precursor. The hydrogenated polysilane was also found to dissolve in solvent mixture of CPS and an organic solvent. The solvent mixture plays an important role in controlling the wettability, coating properties, and thickness of the resulting silicon films, all of which are difficult to control when CPS used alone. In the actual process, UV irradiation is halted before the CPS completely polymerises such that polysilanes of various molecular weights are dissolved in unreacted CPS. By diluting the solution with an organic solvent and then filtering out those insoluble polysilanes that precipitated a result dilution, we obtained the solution that we refer to as "liquid silicon material."

The polymerisation process of CPS was investigated using gel permeation chromatography (GPC). Figure 1 shows the results of the GPC measurements of (a) the CPS and (b) the UV-irradiated CPS. Peaks corresponding to CPS and toluene were observed in both (a) and (b). In addition, in (b) a broad peak was also observed around $M_w=2600$. This peak corresponds to polysilanes of various molecular weights, indicating CPS polymerisation. The GPC measurements were also used to control and optimise the molecular weight distribution of the polysilanes, which significantly affects the wettability of the precursor solution to a glass substrate.

The next step is to form an α -Si film by heating the spin-coated polysilane film to promote its thermal decomposition. Three samples (a), (b) and (c) were prepared to examine the thermal decomposition of the polysilane by thermal desorption spectroscopy (TDS) measurement (see Methods). The relationship between the pre-heating condition of polysilane and the amount of relevant gas— H_2 , SiH_2 and SiH_3 —desorbed during post-annealing of TDS measurements are shown in Figure 2. Sample (a), pre-baked at $300^\circ C$ for 10 minutes, shows a SiH_2 and SiH_3 desorption peak at around $280^\circ C$, followed by intensive hydrogen desorption between $300^\circ C$ and $400^\circ C$, indicating that the polysilane is not completely converted to α -Si when baked at $300^\circ C$ for 10 minutes. Considering the binding energies of Si-Si (224 kJ/mol) and Si-H (318 kJ/mol)²², the Si-Si bonds in the polysilane break first at a temperature lower than $280^\circ C$, followed by the breaking of the Si-H bonds at a higher temperature to start forming a three-dimensional silicon network. In Sample (b), prebaked at $300^\circ C$ for 2 hours, SiH_2 and SiH_3 desorption is three- or four-orders of magnitude lower than that of Sample (a). Sample (c) released much less desorption gas than Samples (a) and (b), since it had almost completely converted to α -Si during pre-heating at $540^\circ C$ for 2 hours. The total amount of hydrogen atoms (atomic ratio of H/Si) in Samples (a), (b) and (c) before TDS measurement are estimated, by TDS analysis, to be more than 22%, 3%, and 0.3%, respectively. Thus, the formation process of α -Si is presumed to be as

follows. As the spin-coated polysilane film is heated, volatile components such as toluene and CPS evaporate first. The Si-Si bonds in the polysilane subsequently start breaking at a temperature below 280°C and a portion of the polysilane is released as SiH₂ and SiH₃. The Si-H bonds start breaking next, at around 300°C, forming a three-dimensional silicon network of α -Si.

We have fabricated simplified bottom gate TFTs using the spin-coated α -Si film to test the electrical properties of the film. The mobility of these α -Si TFTs was 10^{-3} – 10^{-4} cm²V⁻¹s⁻¹ at most. This value is three- or four-orders of magnitude lower comparing the TFTs using α -Si film formed by conventional plasma enhanced chemical vapour deposition (CVD). This poor mobility is attributed to the low concentration of hydrogen atoms that terminate the dangling bonds in the film. Unlike the conventional CVD-formed α -Si film that contains 5–20% hydrogen, the spin-coated α -Si film baked at 540°C for 2 hours contains 0.3% hydrogen and appreciable quantities of dangling bonds to spoil the mobility. On the other hand, the film spin-coated and baked at a low temperature, such as 300°C or lower, contains hydrogen more than 20% and would somewhat function as semiconductor. However, such a low-temperature processed film may not be described as amorphous silicon anymore and is easily oxidized in the air. Some kind of technical solution must be considered to make a good balance between lower process temperature and preventing autoxidation.

Thus, we have investigated the crystallization of the film prior to optimising the low-temperature α -Si process to demonstrate the fundamental potential of the solution process for low-temperature poly-Si (LTPS) TFT applications. Also, low-hydrogen α -Si films are suitable for excimer laser crystallization, which is the standard crystallization method in commercial production of LTPS TFTs²³. The α -Si films formed by coating the liquid silicon material and baking at 540°C were irradiated by a 308-nm XeCl excimer laser at various laser energies. As the laser energy increases, the colour of the

films changed from light auburn to light yellow, suggesting that they were converted to polycrystalline. A TEM image in Figure 3 clearly shows the crystalline growth by laser irradiation. Using Raman spectroscopy²⁴, the laser crystallization behaviours were confirmed to be almost identical to those of conventional CVD-formed α -Si as follows: The full width at half maximum of the crystalline peak in the Raman spectrum decreased sharply as the laser energy increased, reaching a minimum value of 6.3 cm^{-1} at around 300 mJ/cm^2 and thereafter increasing slightly, reflecting microcrystallization.

Next, we have fabricated TFTs using the coating-formed poly-Si films followed by standard fabrication steps used for conventional LTPS TFTs (see Methods). As shown in Fig.4a, these TFTs exhibit good electrical characteristics with field-effect mobility, calculated from the transconductance in the saturation region, ranging from 74 to $108 \text{ cm}^2\text{V}^{-1}\text{s}^{-1}$ in fifteen transistors randomly selected among a 4-inch substrate. The other parameters for the transistors with mobility of $108 \text{ cm}^2\text{V}^{-1}\text{s}^{-1}$ are 7 digits on/off ratio, 5.0 V in V_{th} , and 0.83 V/dec in s-factor.

The mobility was strongly affected not only by the condition of laser crystallization but also by the amount of oxygen in the silicon film. The oxygen concentration was 1100 ppm in the poly-Si film used for the TFTs that exhibited $108 \text{ cm}^2\text{V}^{-1}\text{s}^{-1}$ in mobility. Since the CPS and polysilanes are quite oxygen-sensitive²⁵, several precautions had to be taken during preparation and treatment of a precursor. The coarsely synthesized CPS was distilled repeatedly to remove impurities including oxides before photo-polymerisation. The organic diluent was carefully deoxidised by leaving it in a dry-box for several days before use. The oxygen in the dry-box was strictly kept below 0.5 ppm during all processes from spin-coating to baking. By taking these precautions, we could control the oxygen concentration in the film below 2000 ppm. The TFTs using such low-oxygen films exhibited the mobility as good as 50–100 $\text{cm}^2\text{V}^{-1}\text{s}^{-1}$ and no significant correlation was observed between the oxygen amount and

the mobility since the manufacturing variation such as laser condition is dominant. However, a slight failure in controlling oxygen level in the dry-box yielded a silicon film with the oxygen concentration of 8000 ppm and TFTs with the mobility of $20 \text{ cm}^2\text{V}^{-1}\text{s}^{-1}$ at most. When the oxygen level in the dry-box was intentionally kept at 10 ppm during all processes, α -Si film having 7% of oxygen with insulating behaviour was obtained.

Finally, we demonstrate the printing applicability of the liquid silicon material by fabricating TFTs using ink-jet formation of poly-Si islands (see Methods). The silicon island is the disk-shaped part having a rough surface as shown in the SEM image of Figure 4c. The external disk-shaped part with smooth surface is still unknown, but is presumably the residual remains formed during the drying and shrinking processes of the droplet, which was once spread over the outer disk region. Since the wettability of the liquid silicon material is not understood well enough to control the shrinking phenomena of an ink-jet droplet, the resulting α -Si island became too thick for laser crystallization. A thicker film generally needs higher laser intensity for optimal crystallization. The actual laser intensity used for the crystallization of 60-nm spin-coated and 300-nm ink-jetted Si film was $345\text{mJ}/\text{cm}^2$ and $450\text{mJ}/\text{cm}^2$, respectively. Unlike the former case, the latter intensity is not optimised but roughly determined from its thickness. Using such a intensive laser, surface roughness is easily induced as shown in Fig.4c.

The ink-jetted TFT operated with a mobility of $6.5\text{cm}^2\text{V}^{-1}\text{s}^{-1}$ and on/off ratio of 3 digits as shown in Figure 4a. This low mobility is attributed to the poor crystallinity and the rough surface. The large off current was confirmed to be the current between source and drain, not a leak current thorough gate insulator. This is also attributed to the thick silicon film. Such a thick film contains a lot of dangling bonds and defect near the substrate where crystallization is insufficient. Forming thin and uniform silicon film

using ink-jet process would improve above morphology and electrical properties. However, the wettability and behaviour of micro-droplets are known to be significantly different from those of macroscopic droplets^{26,27}. A thorough understanding of micro-droplets is necessary to realize the ink-jet printing of liquid silicon material for practical applications.

We have demonstrated that high-quality poly-Si film is formed by spin-coating or ink-jetting "liquid silicon material". The mobility of the spin-coated TFT, $108 \text{ cm}^2\text{V}^{-1}\text{s}^{-1}$, is definitely that of a LTPS TFT and cannot be achieved by α -Si TFTs. Though currently inferior to that of conventional and spin-coated LTPS TFT, the performance of the ink-jetted TFT will likely improve along with further advances in both materials and processes. The ultimate goal of this research is to fabricate high-performance silicon TFTs by means of an all-liquid process, wherein all layers are directly patterned with liquid materials. To achieve the goal, we are now trying to develop liquid materials for films other than channel silicon: dielectric layers, doped silicon for source and drain regions, and metallic films for electrodes. The ink-jet process for these liquid materials is also under development. These efforts are expected to establish a novel, low-energy, low-cost and high-throughput process for fabricating high-performance TFTs.

Methods

Preparation and analysis of α -Si film. A 30 vol.% toluene solution of UV-irradiated CPS was spin-coated onto a quartz substrate to yield an approximately 100 nm-thick α -Si film after heat treatment. Heat treatment conditions for Samples (a), (b) and (c) were 300°C for 10 minutes, 300°C for 120 minutes, and 540°C for 120 minutes, respectively, on a hot plate. All these experiments were carried out in a nitrogen-filled dry-box with a residual oxygen concentration of less than 0.5 ppm. The oxygen level in the dry-box was monitored using a galvanic fuel cell sensor. The Raman scattering spectra of these

samples were measured to confirm the α -Si nature of these films at the typical α -Si peak of around 480cm^{-1} . The concentrations of the impurities in these α -Si films were investigated using secondary ion mass spectroscopy (SIMS). The results confirmed that the film was composed almost entirely of silicon, with only a few trace impurities. The alkali and alkali-earth metal impurities, which negatively affect TFT characteristics, were present in less than 1 ppm. The carbon content in the resulting film was surprisingly low—only 200 ppm—considering that an organic solvent was used as a starting material. The oxygen concentration of the film was less than 2000 ppm by strictly controlling the oxygen content in the dry-box to less than 0.5 ppm. Thermal desorption spectroscopy (TDS) was used to investigate the process by which the polysilane is converted to α -Si. In TDS measurement, a sample is heated in a vacuum and the gases that are desorbed from the sample are analysed using mass spectroscopy.

Fabrication of TFTs by spin-coating. The N-channel TFTs, whose structure are schematically illustrated in Figure 4d, were fabricated as follows. First, a SiO_2 underlayer was formed by plasma CVD on a quartz substrate. After cleaning the substrate surface by UV irradiation of 172 nm at $10\text{mW}/\text{cm}^2$ for 10 minutes, the liquid silicon material, 12 vol.% toluene solution of UV-irradiated CPS, was then spin-coated at 2000 rpm in a nitrogen-filled dry-box. The spin-coated substrate was immediately placed on a hot plate heated at 200°C and the temperature was raised to 400°C in 10 minutes. After keeping 400°C for 30 minutes, it was raised again to 540°C in 10 minutes and kept for 2 hours to form a 50-nm-thick α -Si film. Next, the α -Si film was converted into a poly-Si film by 308-nm excimer laser irradiation at $345\text{mJ}/\text{cm}^2$. After the poly-Si was etched to form islands, a 120-nm-thick SiO_2 gate insulator was formed by plasma CVD, followed by tantalum sputtering and etching to form gate electrodes. The source and drain regions were formed by the self-aligned ion implantation of phosphorous ions using the gate electrodes as a mask. Finally, the TFTs became measurable by forming an interlayer insulator, opening contact holes in the insulator to

reveal the source and drain region, and sputtering aluminum to form electrodes. The channel width, W , and channel length, L , of the TFTs were both $10\ \mu\text{m}$. The coating-formed silicon film did not present any notable problems or difficulties during the above fabrication steps, as the silicon film was of semiconductor-grade purity and the film processing conditions—the etching rate, laser conditions, and so forth—were nearly the same as those used for CVD silicon film. Conventional TFTs were also fabricated for comparison by the same process except that the silicon film was formed by CVD.

Fabrication of TFTs by ink-jetting. TFTs with the same structure mentioned above were fabricated using ink-jet printing to form the channel silicon island instead of photolithography. A 10% toluene solution of UV irradiated CPS was ink-jetted on a glass substrate in a nitrogen-filled dry-box. The property of the solution was suitable for ejecting from a piezo-driven print head^{1, 7}. Since the viscosity was almost the same as that of toluene and stability was good enough for months keeping in a dark place at a room temperature, the ejection of the solution from the print head was stable and reproducible. Three droplets having 10 ng in weight were ejected at the place where the channel island was to be formed. The droplets were converted into a poly-Si island having 30–40 μm diameter by baking at 540°C with the same steps used for spin-coated film, followed by 308-nm excimer laser crystallization at $450\text{mJ}/\text{cm}^2$. The island was 300-nm-thick at the centre and become thin toward the peripheral part. The same process as spin-coated TFTs was applied after the gate insulator formation. The channel width, W , and channel length, L , of the TFTs were 36 μm and 2 μm , respectively.

1. Shimoda, T. *et al.* Multicolor pixel patterning of light-emitting polymers by ink-jet printing. *Tech. Digest of SID '99*, 376–379 (1999).
2. Miyashita, S. *et al.* Full color displays fabricated by ink-jet printing. *Proc. of Asia Display/IDW'01*, 1399–1402 (2001).

3. Peumans, P., Uchida, S. & Forrest, S. R. Efficient bulk heterojunction photovoltaic cells using small-molecular-weight organic thin films *Nature* **425**, 158–162 (2003).
4. Okamura, S., Takeuchi, R. & Shiozaki, T. Fabrication of ferroelectric Pb(Zr,Ti)₃ thin films with various Zr/Ti ratios by ink-jet printing. *Jpn. J. Appl. Phys.* **41**, 6714–6717 (2002).
5. Tahar, R. B. H., Ban, T., Ohya, Y. & Takahashi, Y. Optical, structural, and electrical properties of indium oxide thin films prepared by the sol-gel method. *J. Appl. Phys.* **82**, 865–870 (1997).
6. Yudasaka, I., Tanaka, H., Miyasaka, M., Inoue, S. & Shimoda, T. Poly-Si thin-film transistors using polysilazane-based spin-on glass for all dielectric layers. *SID 04 Digest*, 964–967 (2004).
7. Furusawa, M. *et al.* Inkjet-printed bus and address electrodes for plasma display. *Tech. Digest SID'02*, 753–755 (2002).
8. Sirringhaus, H. *et al.* High-resolution inkjet printing of All-polymer transistor circuits. *Science* **290**, 2123–2126 (2000).
9. Kawase, T., Sirringhaus, H., Friend, R. H. & Shimoda, T. All-polymer thin film transistors fabricated by high-resolution ink-jet printing. *Tech. Digest of IEDM*, 623–626 (2000).
10. Gelinck, G. H. *et al.* Flexible active-matrix displays and shift registers based on solution-processed organic transistors. *Nature Materials* **3**, 106–110 (2004).
11. Afzali, A., Dimitrakopoulos, C. D. & Breen, T. L. High-performance, solution-processed organic thin film transistors from a novel pentacene precursor. *J. Am. Chem. Soc.* **124**, 8812–8813 (2002)
12. Ridley, B. A., Nivi, B., Jacobson, J.M. All-inorganic field effect transistors fabricated by printing. *Science* **286**, 746–749 (1999).

13. Mitzi, D. B., Kosbar, L. L., Murray, C. E., Copel, M., Afzali, A. High-mobility ultrathin semiconducting films prepared by spin coating. *Nature* **428**, 299–303 (2004).
14. Aoki, T. *et al.* Method of manufacturing device, device, and electronic apparatus. US Patent Application 2004/0029364.
15. Shimoda, T. *et al.* Method for forming silicon film, US Patent 6541354.
16. Kipping, F. S. Organic derivatives of silicon. Complex silicohydrocarbons $[\text{SiPh}_2]_n$. *J. Chem. Soc.* **125**, 2291–2297 (1924).
17. John, P., Oder, I. M. & Wood, J. The electrical conductivity of polysilane, $(\text{SiH}_2)_x$. *J. Chem. Soc., Chem. Commun.*, 1496–1497 (1983).
18. Suzuki, M., Kotani, J., Gyobu, S., Kaneko, T. & Saegusa, T. Synthesis of sequence-ordered polysilane by anionic ring-opening polymerization of phenylnonamethycyclopentasilane. *Macromolecules* **27**, 2360–2363 (1994).
19. Cypryk, M., Gupta, Y. & Matyjaszewski, K. Anionic ring-opening polymerization of 1,2,3,4-tetramethy-1,2,3,4-tetraphenylcyclotetrasilane. *J. Am. Chem. Soc.* **113**, 1046–1047 (1991).
20. Hengge, E. & Bauer, G. Cyclopentasilan, das erste unsubstituierte cyclische Siliciumhydrid. *Angew. Chem.* **85**, 304–305 (1973).
21. Hengge, E. & Bauer, G. Darstellung und Eigenschaften von Cyclopentasilan. *Monatshefte für Chemie*. **106**, 503–512 (1975).
22. Raabe, G. & Michl, J. Multiple Bonding to Silicon. *Chem. Rev.* **85**, 419–509 (1985).
23. Sameshima, T., Usui, S., & Sekiya, M. XeCl Excimer Laser Annealing Used in the Fabrication of Poly-Si TFTs. *IEEE Electron Device Lett.* **7**, 276–278 (1986).

24. Kitahara, K., Yamazaki, R., Kurosawa, T., Nakajima, K. & Moritani, A. Analysis of stress in laser-crystallized polysilicon thin films by raman scattering spectroscopy. *Jpn. J. Appl. Phys.* **41**, 5055–5059 (2002).
25. Chatgialiloglu, C. *et al.* Autoxidation of Poly(hydrosilane)s. *Organometallics* **17**, 2169–2176 (1998).
26. Morii, K. *et al.* Characterization of light-emitting polymer devices prepared by ink-jet printing. *Proc. 10th Int. Workshop on Inorganic and Organic Electroluminescence* 357–360 (2000).
27. Morii, K., Masuda, T., Ishida, M., Hotta, S., & Shimoda, T. The direct patterning of crystalline organic-semiconductor films on a substrate by ink-jet printing. *Proc. Int. Conference on Synthetic Metals* 126–127 (2004).

Acknowledgements The authors are grateful to the members of Seiko Epson Corporation's pilot line and inkjet industrial application project, for fabricating TFTs and inkjet experiments in this research. This work is partially supported by a grant from the New Energy and Industrial Technology Development Organization (NEDO).

Correspondence and requests for materials should be addressed to M. F. (e-mail: furusawa.masahiro@exc.epson.co.jp).

Figure legends

Figure 1 Gel permeation chromatogram (GPC) of liquid precursor for Si film. **a**, cyclopentasilane (CPS) and **b**, UV-irradiated CPS, both of which were diluted with toluene (1 vol.%) before GPC measurements. The UV irradiation conditions were 405 nm, 100 mW/cm², 10 minutes, for 1 cc of CPS. The broad peak around Mw=2600 corresponds to polysilanes of various molecular weights as a results of the photo-induced polymerisation of CPS.

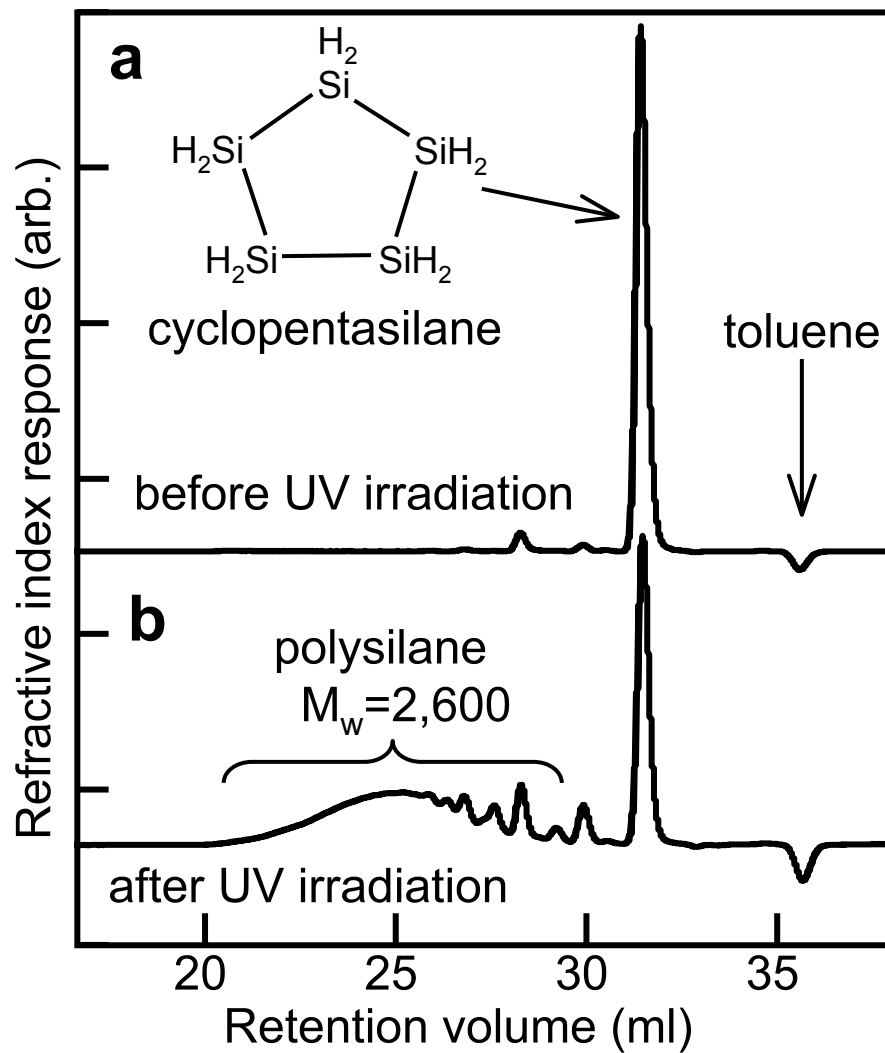
Figure 2 Thermal desorption spectrum (TDS) of solution-processed α -Si film. Three samples were prepared by the thermal decomposition of polysilane at the conditions (**a**) 300°C for 10 minutes, (**b**) 300°C for 120 minutes, (**c**) 540°C for 120 minutes. Desorbed gases from the samples are analysed by mass spectroscopy while the samples are heated in a vacuum.

Figure 3 A TEM image of a solution-processed poly-Si film. The film was formed by spin-coating and baking the liquid silicon materials, followed by laser crystallization. The high-resolution TEM image inserted in the figure clearly highlights the atomic image of the silicon crystal. The micrograph also shows that the grain size in the film is about 300 nm. This grain size is comparable to that of conventional CVD-formed poly-Si film.

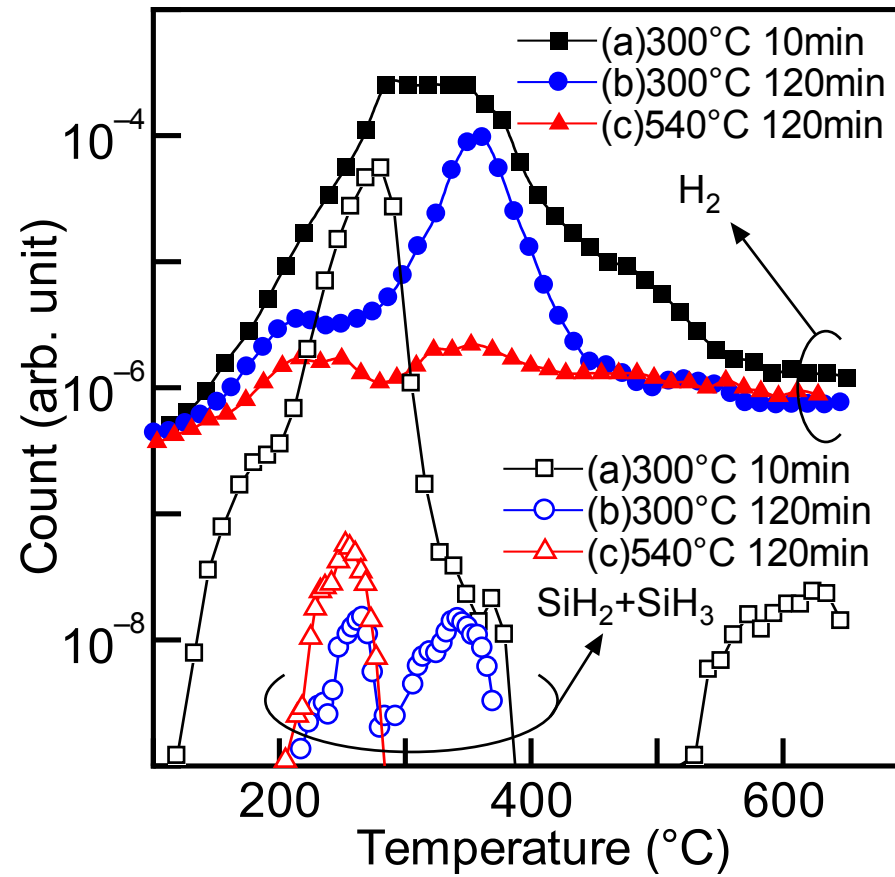
Figure 4 The structures and characteristics of solution-processed LTPS TFT. **a**, The transfer characteristics of LTPS TFTs, whose silicon film was formed by CVD (blue), spin-coating (magenta), and ink-jetting (green), respectively. The drain current of the ink-jetted TFT is normalized to have the same channel width and length as the CVD-formed and spin-coated TFT for comparison. **b**. The output characteristics of the TFT using spin-coated silicon film whose transfer characteristics are shown in **a**. **c**. The SEM

image of the TFT using ink-jetted silicon film whose transfer characteristics are shown in **a. d.** The sectional schematic diagram of a fabricated TFT.

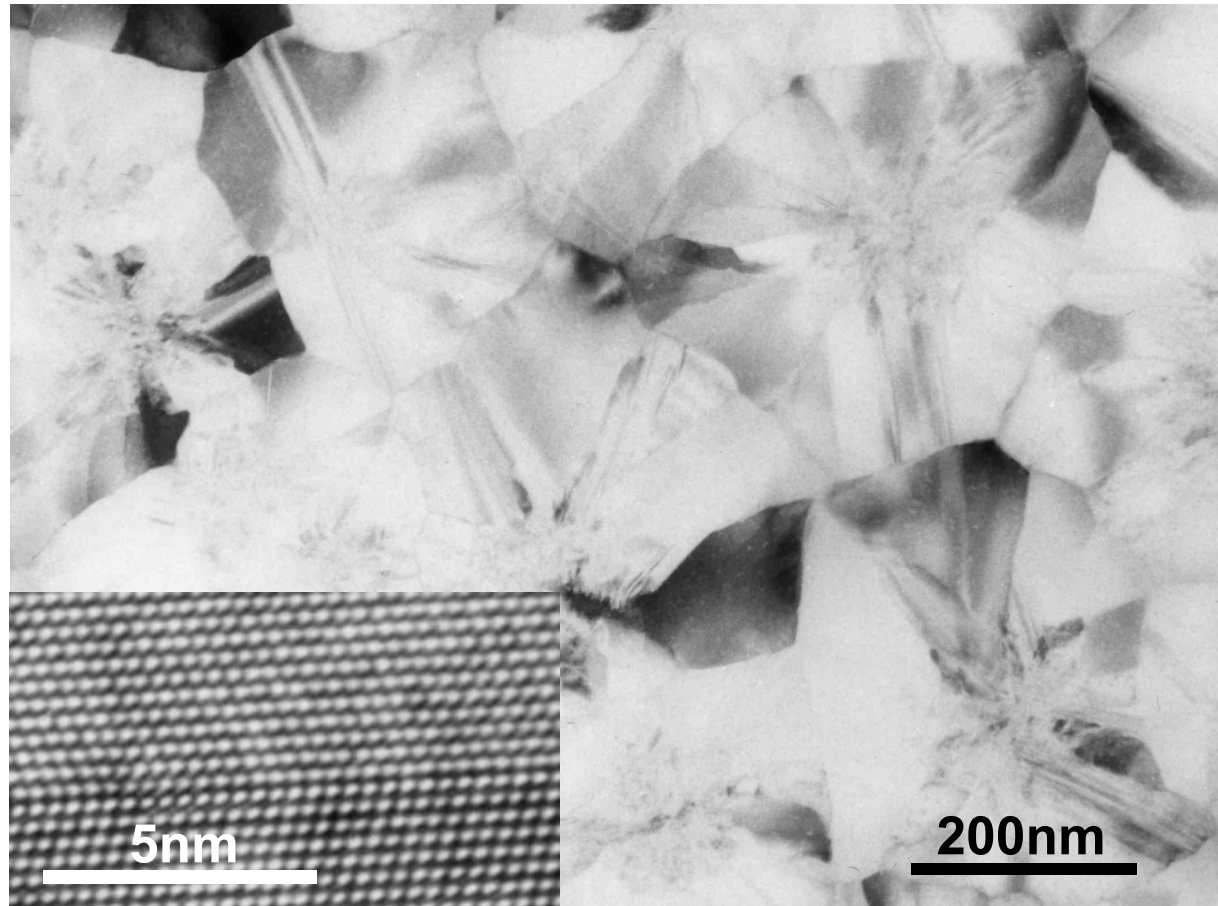
Furusawa(2005-02-02115)Fig.1
Correspondence: furusawa.masahiro@exc.epson.co.jp



Furusawa(2005-02-02115)Fig.2
Correspondence: furusawa.masahiro@exc.epson.co.jp



Furusawa(2005-02-02115)Fig.3
Correspondence: furusawa.masahiro@exc.epson.co.jp



Furusawa(2005-02-02115)Fig.4
Correspondence: furusawa.masahiro@exc.epson.co.jp

